Chapter

Fiber Supercapacitors Based on Carbon Nanotube-PANI Composites

Paa Kwasi Adusei, Yu-Yun Hsieh, Sathya Narayan Kanakaraj, Yanbo Fang, Kevin Johnson, Noe T. Alvarez and Vesselin Shanov

Abstract

Flexible and wearable electronic devices are of a high academic and industrial interest. In order to power these devices, there is a need for compatible energy storage units that can exhibit similar mechanical flexibility. Fiber-based devices have thus become increasingly popular since their light-weight, and flexible structure can be easily integrated into textiles. Supercapacitors have garnered a lot of attention due to their excellent cycling durability, fast charge times and superior power density. The primary challenge, however, with electric double layer capacitors (EDLCs), which are part of the supercapacitor family, is that their energy densities are significantly lower compared to those of batteries. Pseudocapacitors, on the other hand, can be designed and created with large energy densities and other outstanding properties typical for supercapacitors. This chapter discusses the fabrication and testing of supercapacitors based on carbon nanotube-polyaniline (PANI) composite fibers. These flexible and light-weight devices are assembled using different electrolytes for comparison. The created in this work PANI-CNT composite devices attain an energy density of 6.16 Wh/kg at a power density of 630 W/kg and retained a capacitance of 88% over 1000 charge-discharge cycles.

Keywords: pseudocapacitors, CNT Fibers, PANI, fiber supercapacitors

1. Introduction

Over the last few decades there has been an increase in research into energy storage devices arising from the ever increasing energy demands for applications such as portable electronics and electric transportation [1]. Among portable electronics, wearable electronic devices have created a niche for themselves. Fiber-based devices have become increasingly popular since their thread-type structures can be easily integrated into fabrics and other structures.

Supercapacitors are electrochemical energy storage devices that combine the high-energy-storage capability of conventional batteries with the high-power-delivery capability of traditional capacitors [2, 3]. Though they have lower stored energies than batteries, they deliver the stored energy in seconds. Supercapacitors

operate for extended periods of time, often millions of cycles without losing their energy storage capacities giving them an edge over batteries in how long they can be used [4–6].

Supercapacitors have two main classifications that are based on their charge storage mechanism and the type of electrode materials [4]. The first one, electric double layer capacitor (EDLC), stores charges electrostatically on the electrode-electrolyte interfaces of the high surface area carbon materials. This process involves physical adsorption of ions at the electrode and electrolyte interface [2]. The second one, pseudocapacitor, on the other hand, stores charges within the electrodes in response to fast surface and near-surface redox reactions [5, 7]. The electrodes are derived from transition metal oxides and conducting polymers. Due to these redox reactions, pseudocapacitors have been reported with energy densities far higher than that of EDLCs.

With the emergence of flexible electronics such as foldable displays [8], soft photo-detectors [9] and bendable field effect transistors [10], flexible supercapacitors have become more popular than ever. They have been found to be suitable in powering portable and flexible electronic devices, and several have been fabricated with lightweight, flexible and possessing high power and energy densities [11–14]. Planar format supercapacitors have been found to have larger volumes and structural limitations which impede their use in lighter, smaller and omnidirectional flexible electronic devices [15, 16]. To solve these problems, lightweight and high energy density fiber-shaped supercapacitors have been explored and fabricated [17–22].

Fiber electrodes for supercapacitors have been made from active materials with nanostructures, such as CNTs [23–25], graphene [17, 26, 27] and metal oxides [28–30]. However, the most widely studied ones have been CNT fiber electrodes and their composites. This is attributed to CNT's inherent flexibility, high surface area and high electrical conductivity [31]. In their fiber formats, they are highly aligned and have excellent mechanical durability while maintaining all their aforementioned properties.

Polyaniline (PANI) is probably the most widely studied of the conductive polymers because of its high electronic conductivity, redox and ion exchange properties, excellent environmental stability and ease of preparation [32–34]. It has, therefore, been extensively explored in energy storage devices fabricated with pseudocapacitive electrodes.

Bulk PANI, however, due to its low accessible surface area is not ideal for energy storage device electrodes. The workaround to this has been to fabricate nanostructured PANI materials. These structures have typically been made using a carbon template thereby producing materials with a large area to volume ratio and shorter ion diffusion paths [35–37].

In this chapter, we report our high energy density fiber supercapacitors based on CNT-PANI fiber composites. A chemical oxidation polymerization technique is employed to deposit PANI on the surface of the CNT fibers. This composite material gives superior performance as supercapacitor electrodes due to the fast redox reactions between the PANI and the electrolytes used. To create our CNT fibers, we employ a technique that involves dry spinning of multi-walled carbon nanotube (MWCNT) fibers from vertically aligned MWCNT arrays grown by chemical vapor deposition (CVD) as described in a previous publication by our research group [38]. This technique is used to spin continuous fiber at industrial rates from MWCNT arrays of 3 cm width and 4.25 cm length, resulting in fibers with diameters of approximately 55 μm and up to 40 m in length. Next, these fibers underwent atmospheric pressure oxygen plasma functionalization to create oxygen plasma functionalized CNT (OPFCNT) fibers as the base structure for the PANI deposition.

2. Electrode and device fabrication and characterization

2.1 Dry spinning

CNT fibers are dry spun from vertically aligned CNT arrays. In our work, thin films of Fe and Co were sputtered on a silicon wafer, overlaid with approximately 5 nm Al_2O_3 as a buffer layer, by means of physical vapor deposition (PVD). The created structure serves as a catalyst for the growth of aligned CNT arrays on the silicon wafer. This surface-treated substrate was then diced up into required pieces and then exposed to a CVD environment in a FirstNano ET3000 reactor. The resulting CNT array was drawable and spinnable and, by means of twisting and pulling. A homemade setup was used to fabricate highly aligned fibers [38], as shown in **Figure 1**. These pristine CNT fibers, when used to form EDLCs, produce quite low energy densities necessitating the deposition of PANI on them to increase the energy density.

2.2 Oxygen plasma functionalization of fibers

After the fibers were spun, they underwent an atmospheric pressure oxygen plasma functionalization process to improve the wettability of the fibers. This is necessary since carbon-based materials are naturally hydrophobic and need improved wettability to increase the deposition of PANI on the surface of the fiber during the oxidative polymerization process [39–42]. In previous publications [43, 44], carbon-based materials were treated with acids to functionalize them and thereby improve the wettability before polymerization. These involve wet chemistry and as such mostly require multi-step reactions and involve strong chemicals, which affect the bulk properties of the CNT structures. The plasma functionalization process employed in this work is continuous, effective and can be used industrially for extensive lengths of fibers.

Oxygen plasma functionalization was generated by systematically pulling the CNT fiber through a plasma head with a chamber for tubular structures (Surfx Atomflo 400 system). The set-up is shown below in **Figure 2**. The pristine CNT fiber was threaded through the plasma head and affixed to the collector bobbin with double-sided tape. The fiber was pulled through the plasma head at a speed of 0.206 cm/s using the collector bobbin on the motor. This processing led to the functionalization of the fiber with the following plasma parameters: 60 W power, 0.1 L/min oxygen and 15 L/min helium. These parameters were chosen since they ensured the fibers to be functionalized had minimum destruction, checked by Raman spectroscopy.

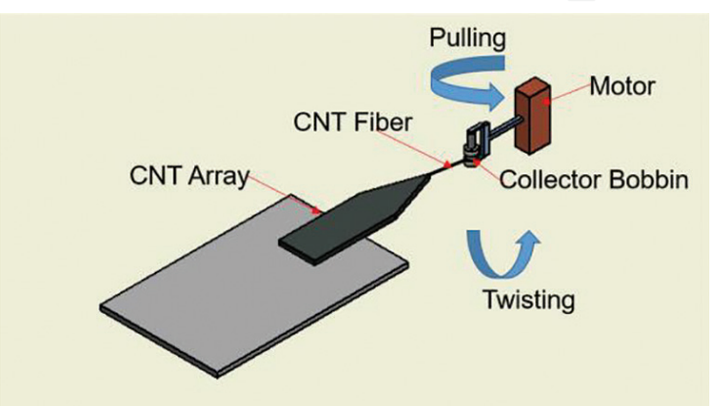

Figure 1.
Carbon nanotube fiber spinning process by twisting and pulling.

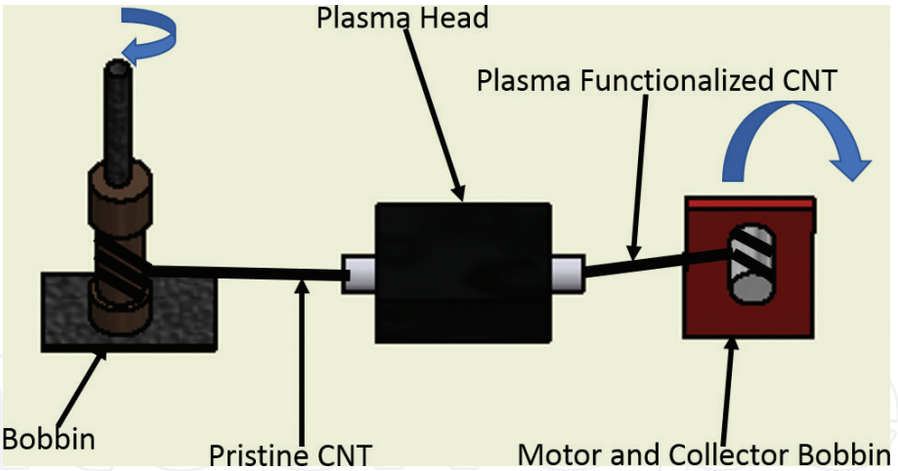

Figure 2.
Oxygen plasma functionalization set-up for CNT fibers.

2.3 Chemical oxidation polymerization

The oxidation of aniline in an acidic aqueous medium using ammonium peroxydisulfate (APS) as an oxidant is widely used and reported in the literature [45, 46]. Emeraldine salt (green color) is the form of PANI obtained during this process [32, 47]. PANI can exist in three oxidation states: leucoemeraldine (fully reduced), emeraldine (partially oxidized) and pernigraniline (fully oxidized) [32, 45–47].

At a pH of less than 2.5, the oxidative polymerization of aniline is a chain reaction [48]. The growth of the chains proceeds by the addition of the monomeric aniline molecules to the active chain ends. The chain growth is terminated after at least one of the reactants in the polymerization runs out. If there is an excess of the APS (oxidant), the resulting polymer remains in the pernigraniline form [49], especially at molar ratios of APS to aniline of over 1.5. If the rate of APS to aniline is equal to 1.25 [50] or aniline is in excess, pernigraniline is reduced to emeraldine at the end of the reaction while aniline is oxidized at the same time to emeraldine [48, 51]. We, therefore, ensured in all our tests that we had excess aniline to promote emeraldine growth, the most thermally and environmentally stable form of PANI [52–54].

The oxygen plasma functionalized CNT (OPFCNT) fibers were cut into 7.5 cm portions and affixed to copper tapes with fast drying silver paint (TedPella Inc.). The copper tapes served as the leads used to connect the devices for electrochemical testing. These electrodes were then placed into 10 ml beakers and put into an ice bath. Aniline monomer dissolved in 1 mol/L HCl and the ammonium persulphate (APS) solution also dissolved in 1 mol/L HCl were then put in the various beakers with fibers at different ratios of aniline to APS. The amount of PANI formed on the fibers was controlled by the ratio of aniline to APS used as well as the time the solution was allowed to polymerize. The fibers were taken out after the polymerization time and rinsed in a beaker with deionized water to wash off the excess PANI.

2.4 Electrode and device fabrication

Fiber supercapacitors were created using poly (vinyl alcohol) and sulfuric acid (PVA-H_2SO_4), as well as polyvinylidene fluoride-co-hexafluoropropylene and 1-ethyl-3-ethylimidazolium (PVDF-EMIMBF4) gel electrolytes. The PVA-H_2SO_4 was made with 10 ml DI water, 2 ml H_2SO_4 and 1 g PVA. The PVDF-EMIMBF4 gel electrolyte was prepared with 15 ml acetone, 1.5 g PVDF, and 3 ml EMIMBF4. The PVA-H_2SO_4 was operated at a 1 V window, while the PVDF-EMIMBF4 was operated at a 3.2 V window. The larger voltage window the PVDF-EMIMBF4 allowed enabled

us to reach larger energy densities. Devices were made from these fibers by coating them with the gel electrolyte (PVA-H_2SO_4 or PVDF-EMIMBF4). The fibers were then placed parallel to each other on a weighing sheet, with more electrolyte and sealed with Kapton tape.

2.5 Electrode and device characterization

Electrochemical measurements were carried out with an electrochemical workstation (Gamry, Interface 1000) at room temperature. The electrochemical characteristics of the electrodes and devices were evaluated by cyclic voltammetry at various scan rates, galvanostatic charge-discharge tests, and electrochemical impedance spectroscopy measurements from 10^6 to 10^{-1} Hz using sinusoidal voltage amplitude of 10 mV at the open circuit potential. In a three-electrode configuration test, Ag/AgCl was used as the reference electrode, platinum served as the counter electrode and the experiments were run in 1 M Na_2SO_4.

The capacitance (C) of the electrodes and fiber supercapacitors was calculated from the galvanostatic discharge curves at different current densities by using the equation: $C=I\Delta t/\Delta V$. The gravimetric capacitance (C_m) and areal capacitance (C_A) were calculated by the following formula: $Cm = C/m$ and $CA = C/A$, respectively. The gravimetric energy density (E_m) and power density (P_m) were calculated by the expressions: $Em = 1/2(Cm(\Delta V)2)/3.6$ and $Pm = 3600Em/t$.$P_m = 3600\frac{E_m}{t}$ The areal energy density (E_A) and power density (P_A) were calculated by the expressions: $EA = 1/2(CA(\Delta V)2)/3.6$ $E_V = \frac{1}{2} * \frac{Cv(\Delta V)^2}{3.6}$ and $PA = 3600EA/t$, $P_V = 3600\frac{E_V}{t}$ where I is the discharge current, t is the discharge time, ΔV is the operating voltage window, m and A refer to the mass and volume of the device, respectively [40, 55].

Scanning electron microscopy (SEM) (FEI XL30, 5 kV) and Raman spectroscopy (Renishaw inVia, 514 nm Ar-ion laser with a laser spot of ~1μm^2) were used to characterize the CNT-PANI. The masses of the fibers were taken on a Sartorius SE2 ultra-microbalance. X-ray photoelectron spectroscopy (XPS) data were obtained using a VG Thermo-Scientific MultiLab 3000 ultra-high vacuum surface analysis system, with ~10^{-9} Torr base pressure using an Al Kα source of 1486.6 eV excitation energy. The high-resolution scans for carbon and low-resolution survey scans were taken for each sample on at least two different locations.

3. Results and discussion

The plasma functionalization of the fiber was confirmed by Raman data **Figure 3a** and XPS data **Figure 3b–d**. From the Raman spectra in **Figure 3a**, we observe an increment in the ratio of intensities between the D and G peak, from 0.776 to 1.195, signifying the destruction of the carbon sp^2 bonds during plasma functionalization. In **Figure 3b**, there is a documented increase in the atomic weight percent of oxygen from 9.1% in the pristine state to 28.17% for the oxygen plasma functionalized thread. **Figure 3c** and **d** is deconvoluted high-resolution C1s and O1s peaks from the XPS data, showing the various oxygen functional groups found on the surface of the fiber which is in close agreement with data reported in the literature [39, 56].

PANI-CNT composite fibers were created from four ratios of aniline to APS (1:1, 2:1, 5:1 and 10:1). The OPFCNT fibers were placed with the chemicals as they polymerized for an hour. From our electrochemical half-cell tests, we observed that a 2:1 aniline to APS ratio gave the best specific capacitance, as seen in **Figure 4a**. Further testing of OPFCNT fibers with varying durations (10 minutes to 6 hours) of polymerization revealed that the composite fibers that

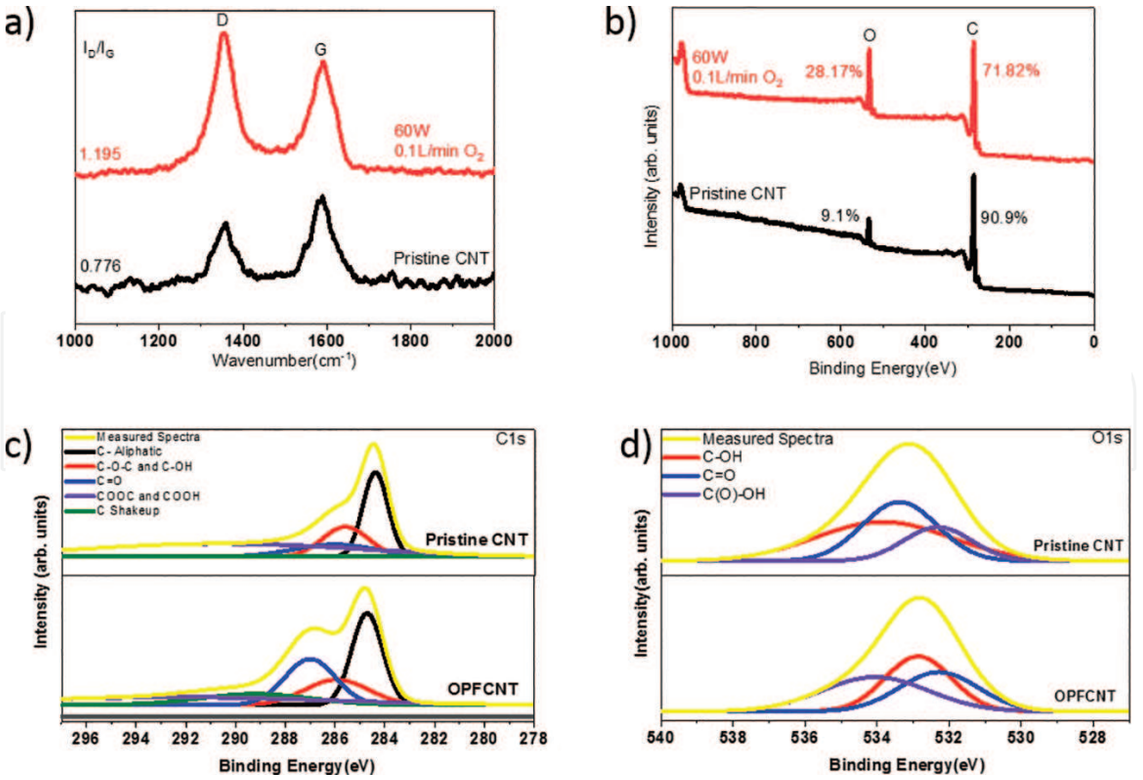

Figure 3.
(a) Raman spectra of pristine and plasma functionalized fiber; (b) XPS survey scans of pristine CNT fiber and plasma functionalized fiber; (c) high-resolution C1s scan of the pristine and plasma functionalized CNT; (d) high-resolution O1s scan of the pristine and plasma functionalized CNT.

underwent polymerization for an hour had the best electrochemistry data, as seen in the inset of **Figure 4a** and in **Figure 4b**. We observed that the polymerization of PANI increased with a higher concentration of APS as well as duration of polymerization. A 1:1 ratio therefore produced more PANI than a 2:1 ratio in the same time frame. PANI in the right amounts improves capacitance of the fibers, however when it becomes deposited in agglomerate morphologies, it leads to the inefficient usage of PANI and reduced capacitance [35–37, 46] . Thus, in the same manner, if polymerization is allowed to take place for longer time these agglomerate morphologies will form and subtract from the synergistic effects of the PANI-CNT composite.

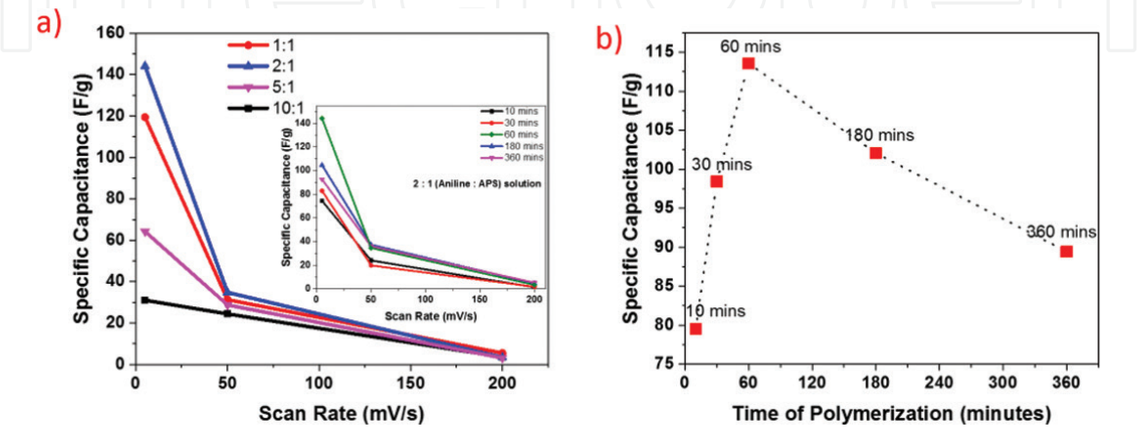

Figure 4.
Half-cell test data for PANI-CNT composite. (a) Specific capacitance vs. scan rates for fibers created at different ratios of aniline to APS for an hour, Inset: specific capacitance vs. scan rate for 2:1 aniline to APS ratio at different times; (b) specific capacitance vs. different times for 2:1 aniline to APS ratio polymerization at 1 A/g.

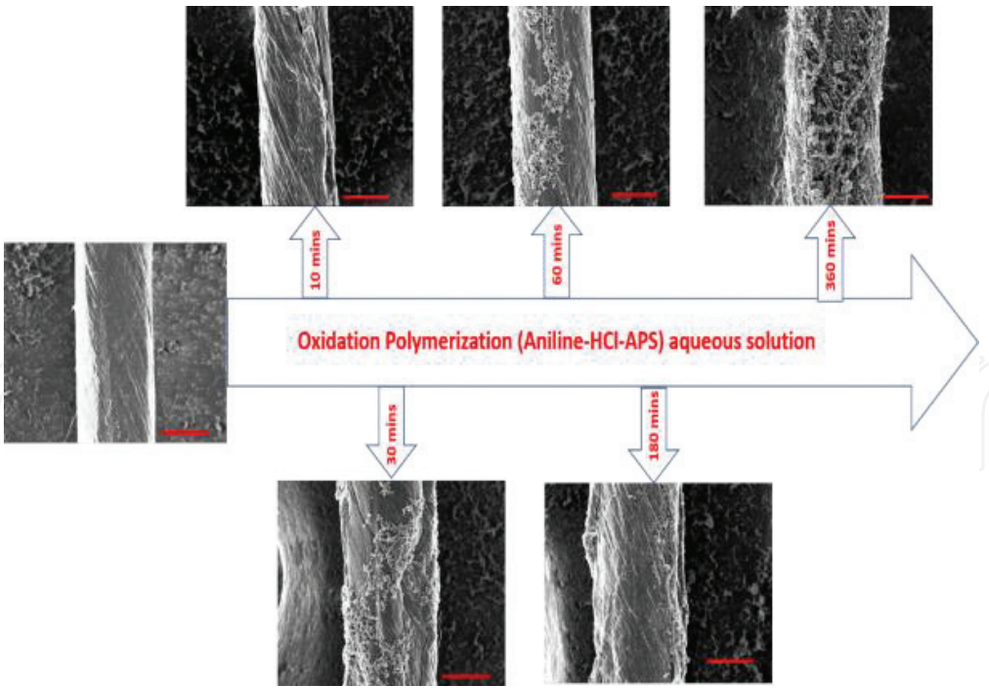

Figure 5.
SEM images showing the route of polymerization of fibers up to 6 hours (magnification 1000, scale: 25 μm).

The structures of the PANI-CNT fibers were observed by SEM. The morphologies and amount of PANI formed were found to correlate strongly to the duration of the polymerization. At 10 minutes, a thin film of PANI forms across the surface of the fiber and as the duration of polymerization increases, PANI nanorods begin to develop in dendritic structures on the fiber. **Figure 5** shows SEM images of the fiber as it progresses from its pristine state to 6 hours of oxidation polymerization.

For ease of referencing, we have labeled the fibers by the number of minutes they were polymerized (minutes-PANI-CNT). **Figure 6** compares pristine CNT, 10-PANI-CNT and 360-PANI-CNT at higher magnifications to reveal the PANI structures being formed. **Figure 6a** shows the pristine fiber which has no PANI on it. In **Figure 6b** we find the onset of the formation of PANI as thin films in the fiber. The agglomerate morphologies of PANI are observed in **Figure 6c**. This shows the increment of PANI morphologies on the surface of the fibers with increasing time for polymerization.

From the Raman data presented in **Figure 7**, we observe the gradual increment in PANI formation on the composite fibers as the duration of polymerization increases. The spectra for pristine CNT and pure PANI are also incorporated, so the gradual transformation from one extreme to the other can be seen. We observe as the duration of polymerization increases the spectra becomes less like CNT and more like PANI.

Devices were created with PANI-CNT fibers, pristine CNT fibers, and OPFCNT fibers. Asymmetrical supercapacitors were also fabricated combining a PANI-CNT fiber and an OPFCNT fiber. The energy density of the PANI-CNT fiber supercapacitor was 3.77 Wh/kg at 0.5 A/g and a power density of about 188 W/kg when using PVA-H_2SO_4. These parameters were dramatically increased to 6.16 Wh/kg and 630 W/kg when using EMIMBF4 corresponding to an almost 64% increment in energy density and 235% increment in power density. **Figure 8** presents a Ragone plot to give a more holistic view of the data as well as a comparison to other previously reported in the literature fiber supercapacitor devices. For ease of comparison, this plot was presented with the areal capacitance, as most fiber supercapacitor data is published with respect to the surface area of the electrodes [57]. The best

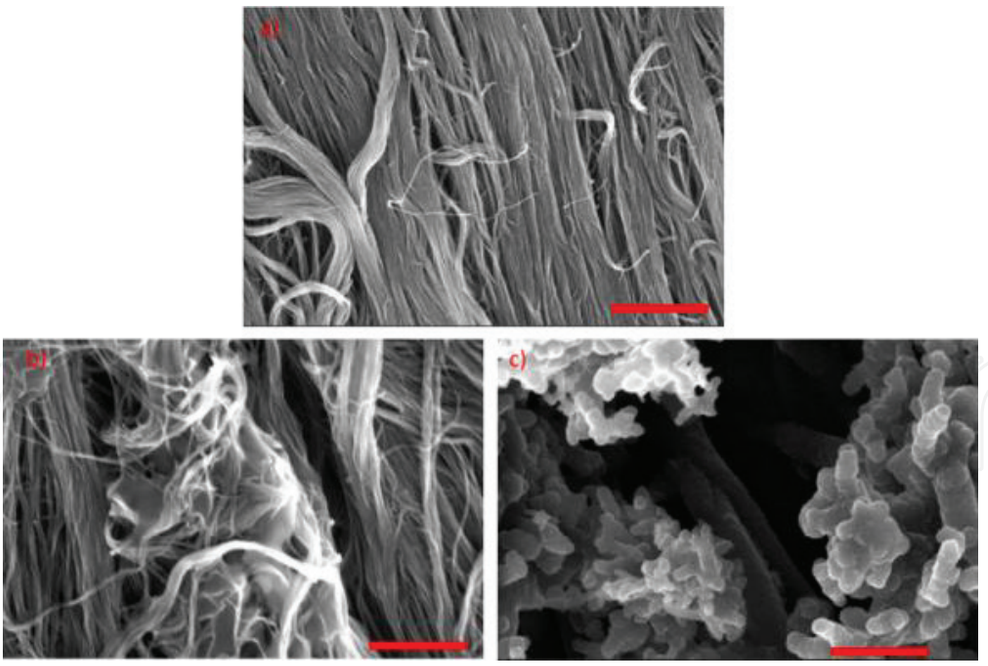

Figure 6.
SEM Images at 25000 magnification (scale: 1 μm). a) Pristine CNT; b)10-PANI-CNT; c) 360-PANI-CNT.

devices (superior energy density and power density) from this Ragone plot were observed in our asymmetric devices. The latter was attributed to the combined redox reactions between the PANI and oxygen functional groups on the surface of the fibers, as well as to the synergistic effect of the pseudocapacitance (PANI-CNT) and EDLC (OPFCNT). Oxygen functional groups have been reported in other works to have improved capacitance of carbon-based materials [58–61] and this also plays a role in the enhanced electrochemical properties of the asymmetrical device.

Figure 9 shows cyclic voltammetry graphs of all the devices at 200 and at 5 mV/s. It can be clearly seen from these graphs that the devices had the characteristic curves

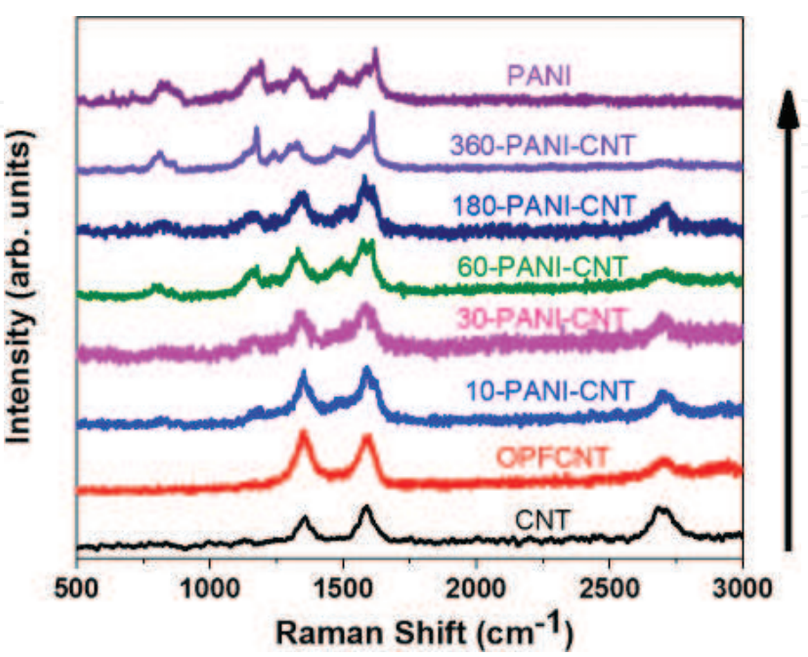

Figure 7.
Raman spectra of CNT, OPFCNT and PANI-CNT composites polymerized at different times.

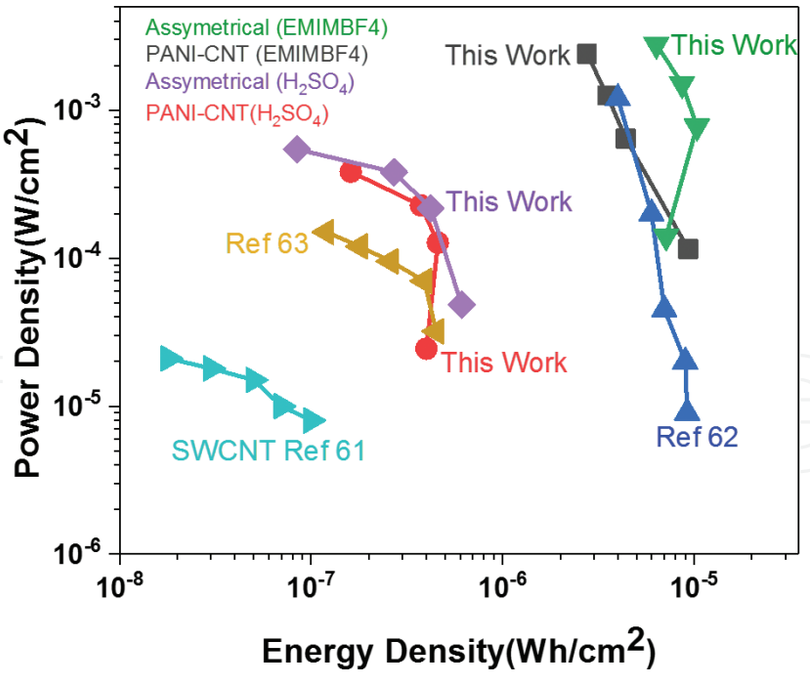

Figure 8.
Ragone plot comparing devices with others in literature [61–63].

of supercapacitors. At lower scan rates (5 mV/s), where redox reactions are more visible, we see larger voltammetry curves for PANI doped threads.

The stability of a supercapacitor is an important parameter since its practical application can be evaluated from this data. **Figure 10** shows the cycling stability of the PANI-CNT (EMIMBF4) device over 1000 cycles. The device retains 88% of its capacitance even after 1000 charge-discharge cycles. This shows good stability and long lifetime of devices.

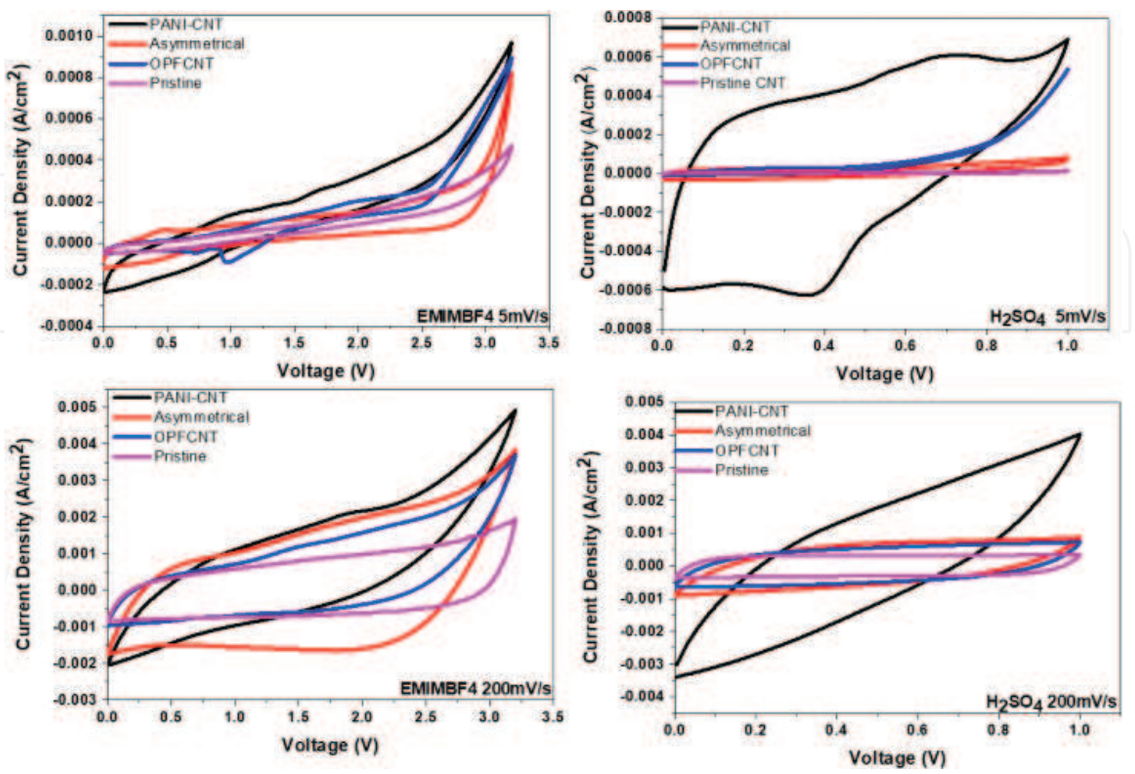

Figure 9.
Cyclic voltammetry curves of devices at 5 and 200 mV/s.

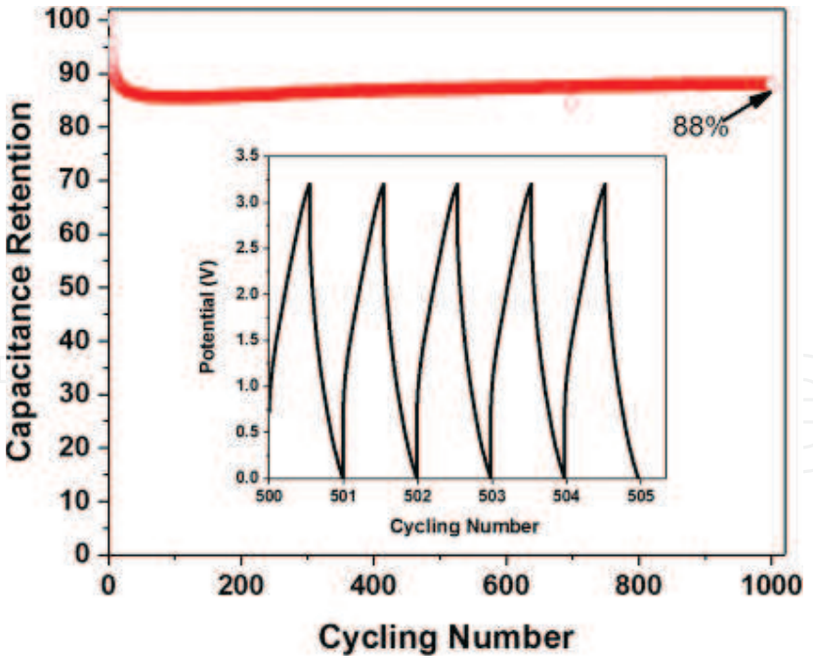

Figure 10.
Cyclic stability for PANI-CNT EMIMBF4 device Inset: galvanostatic charge/discharge curve after 500 cycles.

4. Conclusion

In this chapter, we have discussed the increased attention being given to fiber supercapacitors and their relevance to wearable electronics. We also revealed the role of carbon nanostructured fiber as energy storage devices and the challenges they face. We have successfully synthesized CNT fibers by CVD and dry spinning, applied a post-processing technique to these fibers (oxygen plasma functionalization) and by means of oxidation polymerization doped these fibers with PANI. These fibers were characterized electrochemically, by Raman spectroscopy and with SEM. These fibers were then used as electrodes to create simple fiber devices. The obtained devices produced energy densities of up to 6.16 Wh/kg and 630 W/kg when using EMIMBF4 as electrolytes corresponding to almost a 64% increment in energy density and 335% increment in power density from devices fabricated with PVA-H_2SO_4 (3.77 Wh/kg, 188 W/kg). These devices also maintained excellent capacitance retention (88%) over 1000 charge-discharge cycles. When a comparison was however made with other devices with respect to areal energy density and power density it was observed that the asymmetrical device comprising of an OPFCNT and PANI-CNT showed the best data. This was attributed to the combined redox reactions of both the OPFCNT and PANI-CNT electrodes with the electrolyte.

Acknowledgements

This work was funded by NASA NNX13AF46A and the National Institute for Occupational Safety and Health through the Pilot Research Project Training Program of the University of Cincinnati Education and Research Center Grant # T42OH008432. One of the authors (P. K. A.) would like to thank the Department of Chemical and Environmental Engineering at UC for a partial financial support.

Conflict of interest

The authors declare there is no conflict of interest.

Author details

Paa Kwasi Adusei[1], Yu-Yun Hsieh[1], Sathya Narayan Kanakaraj[1], Yanbo Fang[1], Kevin Johnson[2], Noe T. Alvarez[3] and Vesselin Shanov[1,2]*

1 Department of Mechanical and Materials Engineering, University of Cincinnati, Cincinnati, OH, USA

2 Department of Chemical and Environmental Engineering, University of Cincinnati, OH, USA

3 Department of Chemistry, University of Cincinnati, OH, USA

*Address all correspondence to: vesselin.shanov@uc.edu

References

[1] Bruce PG, Freunberger SA, Hardwick LJ, Tarascon J-M. Li-O_2 and Li-S batteries with high energy storage. Nature Materials. 2012;**11**:19-29. DOI: 10.1038/nmat3191

[2] Burke A. Ultracapacitors: Why, how, and where is the technology. Journal of Power Sources. 2000;**91**:37-50. DOI: 10.1016/S0378-7753(00)00485-7

[3] Conway BE. Electrochemical Supercapacitors: Scientific Fundamentals and Technical Applications; New York: Kluwer Academics/Plenum; 1999

[4] Beidaghi M, Gogotsi Y. Capacitive energy storage in micro-scale devices: Recent advances in design and fabrication of micro-supercapacitors. Energy & Environmental Science. 2014;**7**:867. DOI: 10.1039/c3ee43526a

[5] Simon P, Gogotsi Y. Capacitive energy storage in nanostructured carbon-electrolyte systems. Accounts of Chemical Research. 2013;**46**:1094-1103. DOI: 10.1021/ar200306b

[6] Frackowiak E, Khomenko V, Jurewicz K, Lota K, Béguin F. Supercapacitors based on conducting polymers/nanotubes composites. Journal of Power Sources. 2006;**153**:413-418. DOI: 10.1016/j.jpowsour.2005.05.030

[7] Simon P, Gogotsi Y. Materials for electrochemical capacitors. Nature Materials;**2008,** 7:845-854. DOI: 10.1038/nmat2297

[8] Gelinck GH, Huitema HEA, van Veenendaal E, Cantatore E, Schrijnemakers L, van der Putten JBPH, et al. Flexible active-matrix displays and shift registers based on solution-processed organic transistors. Nature Materials. 2004;**3**:106-110. DOI: 10.1038/nmat1061

[9] Wang X, Song W, Liu B, Chen G, Chen D, Zhou C, et al. High-performance organic-inorganic hybrid photodetectors based on P3HT:CdSe nanowire heterojunctions on rigid and flexible substrates. Advanced Functional Materials. 2013;**23**:1202-1209. DOI: 10.1002/adfm.201201786

[10] Tian B, Cohen-Karni T, Qing Q, Duan X, Xie P, Lieber CM. Three-dimensional, flexible nanoscale field-effect transistors as localized bioprobes. Science (80-). 2010;**329**:830-834. DOI: 10.1126/science.1192033

[11] Lu X, Zhai T, Zhang X, Shen Y, Yuan L, Hu B, et al. WO 3-x@Au@MnO_2 core-shell nanowires on carbon fabric for high-performance flexible supercapacitors. Advanced Materials. 2012;**24**:938-944. DOI: 10.1002/adma.201104113

[12] Huang L, Chen D, Ding Y, Feng S, Wang ZL, Liu M. Nickel-cobalt hydroxide nanosheets coated on $NiCo_2O_4$ nanowires grown on carbon fiber paper for high-performance pseudocapacitors. Nano Letters. 2013;**13**:3135-3139. DOI: 10.1021/nl401086t

[13] Wang X, Liu B, Liu R, Wang Q, Hou X, Chen D, et al. Fiber-based flexible all-solid-state asymmetric supercapacitors for integrated photodetecting system. Angewandte Chemie, International Edition. 2014;**53**:1849-1853. DOI: 10.1002/anie.201307581

[14] Liu B, Zhang J, Wang X, Chen G, Chen D, Zhou C, et al. Hierarchical three-dimensional $ZnCo_2O_4$ nanowire arrays/carbon cloth anodes for a novel class of high-performance flexible lithium-ion batteries. Nano Letters. 2012;**12**:3005-3011. DOI: 10.1021/nl300794f

[15] Chen T, Yang Z, Peng H. Integrated devices to realize energy conversion and storage simultaneously. Chemphyschem. 2013;**14**:1777-1782. DOI: 10.1002/cphc.201300032

[16] Wang X, Lu X, Liu B, Chen D, Tong Y, Shen G. Flexible energy-storage devices: Design consideration and recent progress. Advanced Materials. 2014;**26**:4763-4782. DOI: 10.1002/adma.201400910

[17] Meng Y, Zhao Y, Hu C, Cheng H, Hu Y, Zhang Z, et al. All-graphene core-sheath microfibers for all-solid-state, stretchable fibriform supercapacitors and wearable electronic textiles. Advanced Materials. 2013;**25**:2326-2331. DOI: 10.1002/adma.201300132

[18] Liu B, Tan D, Wang X, Chen D, Shen G. Flexible, planar-integrated, all-solid-state fiber supercapacitors with an enhanced distributed-capacitance effect. Small. 2013;**9**:1998-2004. DOI: 10.1002/smll.201202586

[19] Xiao X, Li T, Yang P, Gao Y, Jin H, Ni W, et al. Fiber-based all-solid-state flexible supercapacitors for self-powered systems. ACS Nano. 2012;**6**:9200-9206. DOI: 10.1021/nn303530k

[20] Le VT, Kim H, Ghosh A, Kim J, Chang J, Vu QA, et al. Coaxial fiber supercapacitor using all-carbon material electrodes. ACS Nano. 2013;**7**:5940-5947. DOI: 10.1021/nn4016345

[21] Fu Y, Cai X, Wu H, Lv Z, Hou S, Peng M, et al. Fiber supercapacitors utilizing pen ink for flexible/wearable energy storage. Advanced Materials. 2012;**24**:5713-5718. DOI: 10.1002/adma.201202930

[22] Xu P, Gu T, Cao Z, Wei B, Yu J, Li F, et al. Carbon nanotube fiber based stretchable wire-shaped supercapacitors. Advanced Energy Materials. 2014;**4**:1300759(1-6). DOI: 10.1002/aenm

[23] Wang K, Meng Q, Zhang Y, Wei Z, Miao M. High-performance two-ply yarn supercapacitors based on carbon nanotubes and polyaniline nanowire arrays. Advanced Materials. 2013;**25**:1494-1498. DOI: 10.1002/adma.201204598

[24] Ren J, Li L, Chen C, Chen X, Cai Z, Qiu L, et al. Twisting carbon nanotube fibers for both wire-shaped micro-supercapacitor and micro-battery. Advanced Materials. 2013;**25**:1155-1159. DOI: 10.1002/adma.201203445

[25] Su F, Miao M, Niu H, Wei Z. Gamma-irradiated carbon nanotube yarn as substrate for high-performance fiber supercapacitors. ACS Applied Materials & Interfaces. 2014;**6**:2553-2560. DOI: 10.1021/am404967x

[26] Zhao X, Zheng B, Huang T, Gao C. Graphene-based single fiber supercapacitor with a coaxial structure. Nanoscale. 2015;**7**:032001-20. DOI: 10.1039/c5nr01737h

[27] Aboutalebi SH, Jalili R, Esrafilzadeh D, Salari M, Gholamvand Z, Yamini SA, et al. High-performance multifunctional graphene yarns: Toward wearable all-carbon energy storage textiles. ACS Nano. 2014;**8**:2456-2466. DOI: 10.1021/nn406026z

[28] Su F, Miao M. Asymmetric carbon nanotube–MnO_2 two-ply yarn supercapacitors for wearable electronics. Nanotechnology. 2014;**25**:135401. DOI: 10.1088/0957-4484/25/13/135401

[29] Choi C, Kim SH, Sim HJ, Lee JA, Choi AY, Kim YT, et al. Stretchable, weavable coiled carbon nanotube/MnO_2/polymer fiber solid-state supercapacitors. Scientific Reports. 2015;**5**:1-6. DOI: 10.1038/srep09387

[30] Bae J, Park YJ, Lee M, Cha SN, Choi YJ, Lee CS, et al. Single-fiber-based hybridization of energy converters

and storage units using graphene as electrodes. Advanced Materials. 2011;**23**:3446-3449. DOI: 10.1002/adma.201101345

[31] Chen T, Qiu L, Kia HG, Yang Z, Peng H. Designing aligned inorganic nanotubes at the electrode interface: Towards highly efficient photovoltaic wires. Advanced Materials. 2012;**24**:4623-4628. DOI: 10.1002/adma.201201893

[32] Sapurina I, Stejskal J. The mechanism of the oxidative polymerization of aniline and the formation of supramolecular polyaniline structures. Polymer International. 2008;**57**:1295-1325. DOI: 10.1002/pi

[33] Gospodinova N, Terlemezyan L. Conducting polymers prepared by oxidative polymerization: Polyaniline. Progress in Polymer Science. 1998;**23**:1443-1484. DOI: 10.1016/S0079-6700(98)00008-2

[34] Syed AA, Dinesan MK. Review: Polyaniline-A novel polymeric material. Talanta. 1991;**38**:815-837. DOI: 10.1016/0039-9140(91)80261-W

[35] Simotwo SK, Delre C, Kalra V. Supercapacitor electrodes based on high-purity electrospun polyaniline and polyaniline-carbon nanotube nanofibers. ACS Applied Materials & Interfaces. 2016;**8**:21261-21269. DOI: 10.1021/acsami.6b03463

[36] Wang X, Liu D, Deng J, Duan X, Guo J, Liu P. Improving cyclic stability of polyaniline by thermal crosslinking as electrode material for supercapacitors. RSC Advances. 2015;**5**:78545-78552. DOI: 10.1039/C5RA17327B

[37] Cho S, Shin K-H, Jang J. Enhanced electrochemical performance of highly porous supercapacitor electrodes based on solution processed polyaniline thin films. ACS Applied Materials & Interfaces. 2013;**5**:9186-9193. DOI: 10.1021/am402702y

[38] Alvarez NT, Miller P, Haase M, Kienzle N, Zhang L, Schulz MJ, et al. Carbon nanotube assembly at near-industrial natural-fiber spinning rates. Carbon N Y. 2015;**86**:350-357. DOI: 10.1016/j.carbon.2015.01.058

[39] Malik R, Mcconnell C, Alvarez NT, Haase M, Shanov V. RSC advances rapid, in situ plasma functionalization of carbon nanotubes for improved CNT/epoxy composites. RSC Advances. 2016;**6**:108840-108850. DOI: 10.1039/C6RA23103A

[40] Zhang L, DeArmond D, Alvarez NT, Malik R, Oslin N, McConnell C, et al. Flexible micro-supercapacitor based on graphene with 3D structure. Small. 2017;**13**:1-10. DOI: 10.1002/smll.201603114

[41] Lobo AO, Ramos SC, Antunes EF, Marciano FR, Trava-Airoldi VJ, Corat EJ. Fast functionalization of vertically aligned multiwalled carbon nanotubes using oxygen plasma. Materials Letters. 2012;**70**:89-93. DOI: 10.1016/j.matlet.2011.11.071

[42] Yu H, Cheng D, Williams TS, Severino J, De Rosa IM, Carlson L, et al. Rapid oxidative activation of carbon nanotube yarn and sheet by a radio frequency, atmospheric pressure, helium and oxygen plasma. Carbon N Y. 2013;**57**:11-21. DOI: 10.1016/j.carbon.2013.01.010

[43] Ramana GV, Srikanth VVSS, Padya B, Jain PK. Carbon nanotube-polyaniline nanotube core-shell structures for electrochemical applications. European Polymer Journal. 2014;**57**:137-142. DOI: 10.1016/j.eurpolymj.2014.05.018

[44] Zhang Y, Cui X, Zu L, Cai X, Liu Y, Wang X, et al. New supercapacitors based on the synergetic redox effect

between electrode and electrolyte. Materials (Basel). 2016;**9**:1-13. DOI: 10.3390/ma9090734

[45] Lim YJ, Park MY, Lee SK, Lee WK, Jo NJ. Polyaniline and multi-walled carbon nanotube composite electrode for rechargeable battery. Transactions of the Nonferrous Metals Society of China (English Ed). 2012;**22**:s717-s721. DOI: 10.1016/S1003-6326(12)61793-2

[46] Wang H, Lin J, Shen ZX. Polyaniline (PANi) based electrode materials for energy storage and conversion. Journal of Science: Advanced Materials and Devices. 2016;**1**:225-255. DOI: 10.1016/j.jsamd.2016.08.001

[47] Simotwo SK, Kalra V. Polyaniline-based electrodes: Recent application in supercapacitors and next generation rechargeable batteries. Current Opinion in Chemical Engineering. 2016;**13**:150-160. DOI: 10.1016/j.coche.2016.09.001

[48] Stejskal J, Kratochvíl P, Jenkins AD. The formation of polyaniline and the nature of its structures. Polymer (Guildf). 1996;**37**:367-369. DOI: 10.1016/0032-3861(96)81113-X

[49] Manohar SK, Macdiarmid AG, Epstein AJ. Polyaniline: Pernigranile, an isolable intermediate in teh conventional chemical synthesis of emeraldine. Synthetic Metals. 1991;**41**:711-714. DOI: 10.1016/0379-6779(91)91165-7

[50] Stejskal J, Gilbert RG. Polyaniline. Preparation of a conducting polymer (IUPAC Technical Report). Pure and Applied Chemistry. 2002;**74**:857867. DOI: 10.1351/pac200274050857

[51] Kolla HS, Surwade SP, Zhang X, MacDiarmid AG, Manohar SK. Absolute molecular weight of polyaniline. Journal of the American Chemical Society. 2005;**127**:16770-16771. DOI: 10.1021/ja055327k

[52] Brožová L, Holler P, Kovářová J, Stejskal J, Trchová M. The stability of polyaniline in strongly alkaline or acidic aqueous media. Polymer Degradation and Stability. 2008;**93**:592-600. DOI: 10.1016/j.polymdegradstab. 2008.01.012

[53] Blinova NV, Sapurina I, Klimovič J, Stejskal J. The chemical and colloidal stability of polyaniline dispersions. Polymer Degradation and Stability. 2005;**88**:428-434. DOI: 10.1016/j.polymdegradstab. 2004.11.014

[54] Prokeš J, Stejskal J. Polyaniline prepared in the presence of various acids: 2. Thermal stability of conductivity. Polymer Degradation and Stability. 2004;**86**:187-195. DOI: 10.1016/j.polymdegradstab. 2004.04.012

[55] Owusu KA, Qu L, Li J, Wang Z, Zhao K, Yang C, et al. Low-crystalline iron oxide hydroxide nanoparticle anode for high-performance supercapacitors. Nature Communications. 2017;**8**:1-11. DOI: 10.1038/ncomms14264

[56] Zschoerper NP, Katzenmaier V, Vohrer U, Haupt M, Oehr C, Hirth T. Analytical investigation of the composition of plasma-induced functional groups on carbon nanotube sheets. Carbon N Y. 2009;**47**:2174-2185. DOI: 10.1016/j.carbon.2009.03.059

[57] Gogotsi Y, Simon P. True performance metrics in electrochemical energy storage. Materials Science. 2011;**334**:917-918. DOI: 10.1126/science.1213003

[58] Nian YR, Teng H. Influence of surface oxides on the impedance behavior of carbon-based electrochemical capacitors. Journal of Electroanalytical Chemistry. 2003;**540**:119-127. DOI: 10.1016/S0022-0728(02)01299-8

[59] Hsieh CT, Teng H. Influence of oxygen treatment on electric double-layer capacitance of activated carbon fabrics. Carbon N Y. 2002;**40**:667-674. DOI: 10.1016/S0008-6223(01)00182-8

[60] Centeno TA, Stoeckli F. On the specific double-layer capacitance of activated carbons, in relation to their structural and chemical properties. Journal of Power Sources. 2006;**154**:314-320. DOI: 10.1016/j.jpowsour.2005.04.007

[61] Meng J, Nie W, Zhang K, Xu F, Ding X, Wang S, et al. Enhancing electrochemical performance of graphene fiber-based supercapacitors by plasma treatment. ACS Applied Materials & Interfaces. 2018::acsami.8b04438. DOI: 10.1021/acsami.8b04438

[62] Huang Y, Hu H, Huang Y, Zhu M, Meng W, Liu C, et al. From industrially weavable and knittable highly conductive yarns to large wearable energy storage textiles. ACS Nano. 2015;**9**:4766-4775. DOI: 10.1021/acsnano.5b00860

[63] Meng Q, Wang K, Guo W, Fang J, Wei Z, She X. Thread-like supercapacitors based on one-step spun nanocomposite yarns. Small. 2014;**10**:3187-3193. DOI: 10.1002/smll.201303419